Significance of Secondary Ion Mass Spectrometry Microscopy for Technetium-99m Mapping in Leukocytes

C. Fourré, S. Halpern, J. Jeusset, J. Clerc and P. Fragu

INSERM U66 Equipe de Microscopie Ionique: Relation Imagerie Chimique Quantitative-Fonctions Cellulaires, Institut Gustave-Roussy, Villejuif et Service de Médecine Nucléaire, Hopital Kremlin-Bicêtre, France

Secondary ion mass spectrometry (SIMS) microscopy is the only method potentially capable of mapping all the elements in the periodic table including stable and radioactive isotopes. We used this method to study ^{99m}Tc distribution by detecting and localizing of ^{99}Tc, a daughter product which has the same mass and the same chemical properties. It was combined with albumin macroaggregates or with Hexamethylpropyleneamine oxime (HMPAO) in leukocytes. The efficiency of ^{99}Tc ionization under Cs^+ bombardment was higher than with an O_2^+ beam. By using high mass resolution we succeeded in detecting and localizing ^{99}Tc in cell sections by eliminating polyatomic ions that arise from this biological matrix. The ^{99}Tc specific signal was obtained with a mass resolution of 2000 for labeled albumin macroaggregates, and 5000 for HMPAO-labeled leukocytes. In the latter, the labeling varied from one cell to another and ^{99}Tc was present in both the nucleus and the cytoplasm. The results indicate that SIMS microscopy can provide new insights into ^{99m}Tc dosimetry.

J Nucl Med 1992; 33:2162–2166

Knowledge of how radioligands used for diagnosis and/or therapy are distributed in human tissue is an essential prerequisite for dosimetry studies in nuclear medicine. Microautoradiography is a technique usually employed to image radioisotope distribution but conventional emulsions are only able to use radioisotopes which emit ionizing particles (α, β, or electrons). Lateral resolution, which may also be a limiting factor in element localization, is dependent on the energy of the ionizing particle. This imposes a further restriction on the choice of isotope (*1,2*). Yet another drawback is the prolonged duration of exposure to ionizing particles which can last several days. Microanalytical methods such as electron probe x-ray microanalysis and electron energy loss spectrometry (*3,4*), can detect and quantify chemical elements but are generally incapable of imaging low concentrations or physiological elements in tissue. Moreover, these methods cannot be used to distinguish between stable and radioactive isotopes of a given element. An alternative approach is provided by secondary ion mass spectrometry (SIMS) microscopy. This technique is the only one capable of mapping all the elements in the periodic table, including stable and radioactive isotopes. Its usefulness for the study of the constitutive chemical elements of cells is now well established (*5–10*).

We used SIMS microscopy to study ^{99m}Tc in tissue sections. Technetium used for labeling in nuclear medicine in a mixture of ^{99m}Tc and ^{99}Tc, both of which vary in proportion according to the time between two elutions. Whereas in nuclear medicine ^{99m}Tc should be as large as possible in order to be detected, this is not necessary in SIMS because both ^{99m}Tc and diexcited ^{99}Tc can be visualized in a same signal without any limitations on the proportion present after elution. We report here our study of the distribution in tissue specimens of ^{99}Tc, combined with the ligand hexamethylpropyleneaminoxime (HMPAO). This lipophilic complex labels isolated leukocytes, which are then used to explore infectious sites in humans (*11*). Our results indicate that SIMS microscopy can provide new insights into ^{99m}Tc dosimetry by identifying the cellular distribution of the ^{99}Tc.

MATERIALS AND METHODS

SIMS Microscopy

Principle. Figure 1 shows the principle of SIMS microscopy. A primary ion beam is focused onto the surface of a resin-embedded biological tissue section. Under ion bombardment the atoms of the most superficial molecular layers (1–5 nm) of the specimen are progressively sputtered and some of them are ionized. These secondary ions, either single or polyatomic ions, characteristic of the atomic composition of the area analyzed, are focused and energy filtered. The various ion species are separated by a mass spectrometer. An analytical image of the selected element is displayed on a fluorescent screen. An electron multiplier measures the intensity of this selected secondary ion beam. These secondary ions can also be displayed as mass spectra at various mass resolutions according to the instrument used. The instrument in our study was the Cameca IMS 3F (Cameca, France)

Received Mar. 6, 1992; revision accepted Jul. 1, 1992.

For reprints contact: Catherine Fourré, INSERM U66, Institut Gustave-Roussy, 94800 Villejuif, France.

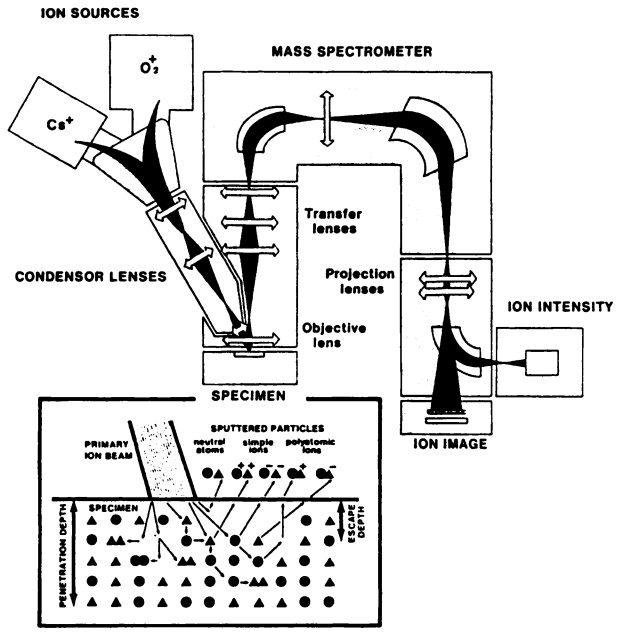

FIGURE 1. Diagram of SIMS microscope Cameca IMS 3F.

fitted with an O_2^+ or Cs^+ primary ion source. This instrument was specially designed to obtain images with high mass resolution. In SIMS, the mass resolution is expressed by M/ΔM (M = studied mass and M/ΔM = the smallest differential mass that can be distinguished); mass resolution is obtained by opening or closing mass spectrometer splits. When the mass resolution is high, the sensitivity decreases. In practice, the mass resolution can be adjusted from 200 to 10,000 and we studied mass spectra at several resolutions. The lateral resolution is 0.5 μm. The analyzed area varied from 1.5 to 400 μm in diameter.

Mass Spectra. When studying biological tissue, reference samples of the same nature should be used to determine the mass resolution required to eliminate polyatomic ion interferences (*12,13*). During sample sputtering, some ionized atoms are emitted as polyatomic ions which are specific to the matrix but are also a source of artifact signals. In polyatomic ions, the number of nucleons is identical to that found in a single element with the same nominal mass, but due to a mass defect the polyatomic ions are heavier and do not follow the same trajectory in the spectrometer as a single element. Mass spectra were obtained with a low current 10 keV Cs^+ primary beam (20–30 nA) on areas of 60 μm in diameter.

Elemental Imaging. Direct electronegative ion imaging was performed with a low current 10 keV Cs^+ primary beam (20–30 nA) focused on areas of 60 and 150 μm in diameter. A sensitive S.I.T. video camera (LHESA SIT 4036) linked to an image processing system was used to obtain high speed signal integration which improved the signal-noise ratio. Image integration times were optimized for the quality of the image but were not representative of local element concentration. On-line and off-line superimpositions in pseudocolors of two and three ion images respectively were used to obtain a composite image which was easier to interpret (*14*). Pseudocolored images on the colored screen were photographed with 100 ASA Tura film.

Protocol

$^{99}TcO_4^-NH_4^+$ Standard. In order to set up the ^{99}Tc mass in the mass spectrometer, 18.5 MBq (0.5 mCi) of $^{99}TcO_4^-NH_4^+$ were embedded in methacrylate resin (Historesin, Pharmacia, Uppsala, Sweden) and semithin sections (3 μm) were prepared.

Technetium-99 Reference Sample. The second step in the procedure used to detect ^{99}Tc was to prepare a biological reference sample rich in this element to determine the mass resolution necessary to obtain the ^{99}Tc signal. Human albumin macroaggregates (AMA) (TCK-8, kit CIS, Gif sur Yvette, France) were selected because they had a similar matrix to that of the biological

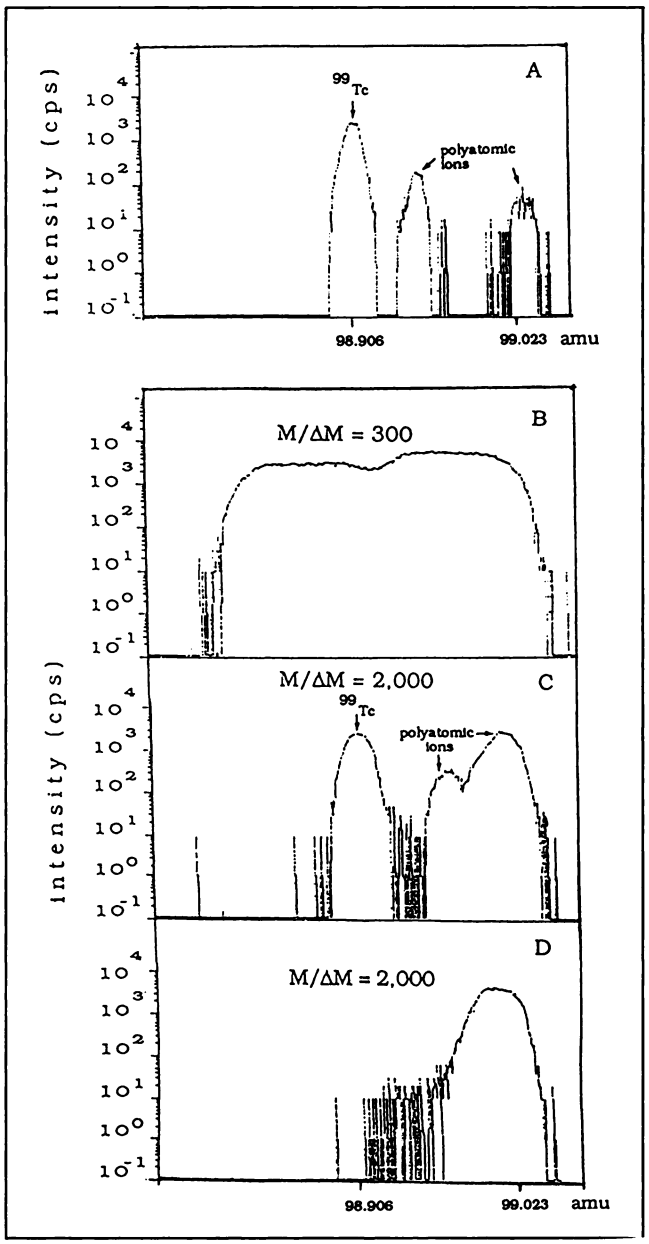

FIGURE 2. Technetium-99 detection. The mass spectra obtained from the $^{99}TcO_4^-NH_4^+$ sample allowed us to set the mass spectrometer at the 98.906 amu (A). Mass spectra of ^{99}Tc bound to albumin macroaggregates were obtained with variable mass resolutions: (B) low mass resolution and (C) high mass resolution. No ^{99}Tc signal was detected on AMA without ^{99}Tc (D).

sample and because of their high labeling efficiency (>90% for ^{99m}Tc activity below 100 mCi). The labeling technique described by the manufacturer was used. In order to obtain a large amount of technetium atoms, we used a pertechnetate solution obtained from the generator which was not eluted for 72 hr. Of this solution, 24 GBq (650 mCi) were added to 2 mg of AMA, and incubated at room temperature for 5 min. The suspension was centrifuged at 200 g for 10 min and the AMA pellet was fixed in a solution containing 1 g/l glutaraldehyde and 20 g/l paraformaldehyde in cacodylate buffer (0.1 *M* pH 7.4). Fragments were dehydrated in ethanol and embedded in methacrylate resin. Semithin sections (3 μm) were deposited on ultrapure gold holders for ion analysis.

A negative control was prepared in the same manner but the pertechnetate solution was replaced by NaCl (0.9%). The ^{99m}Tc labeling yield, determined by centrifugation of the AMA suspension and pellet counting, was 87% for ^{99m}Tc and the same for ^{99}Tc. Less than 2% of radioactivity (estimated by counting supernatants after washing) was lost during sample preparation for SIMS microscopy.

Technetium-99-Leukocyte Labeling. Three leukocyte pellets were prepared: the first for ^{99m}Tc-HMPAO labeling (Pellet 1), the second for HMPAO labeling without ^{99m}Tc (Pellet 2) and the third was not labeled (Pellet 3). A 90 ml sample of human blood was drawn with three sterile heparinized syringes and transferred to three conical plastic tubes. Sediments were obtained 70 to 90 min after the addition of 30 ml dextran to each tube. The leukocyte-rich plasma was removed and centrifuged at 200 g for 10 min. Red cells were eliminated by resuspending the pellet in 2 ml of distilled water for 1 min with gentle shaking. The suspension was made isotonic by adding 2 ml NaCl (1.8%) and was centrifuged at 200 g for 10 min. Pellet 1 was incubated with 1.1 GBq (30 mCi) of freshly prepared ^{99m}Tc-HMPAO (CERETEC, Amersham) for 10 min at 20°C. Pellet 2 was incubated with HMPAO without ^{99m}Tc for 10 min at 20°C. The three pellets were washed with 5 ml NaCl (0.9%), centrifuged at 200 g for 10 min and fixed as described for the reference sample.

For cells the labeling yield and activity loss, estimated by same AMA protocol, were 50% and 5% respectively.

RESULTS

Technetium-99 Detection

Figure 2A shows mass spectra obtained with a $^{99}TcO_4^-NH_4^+$ standard section. An O_2^+ or Cs^+ primary ion beam was used on this sample to determine the best conditions for measuring secondary ^{99}Tc emissions. The Cs^+ primary ion beam was chosen because it ionized the Tc more efficiently than the O_2^+ beam.

Mass Resolution

The ^{99}Tc reference sample was used to determine the mass resolution required to eliminate polyatomic ion interferences. Figure 2B–D shows mass spectra obtained for a mass resolution ranging from 300 to 2000 and the change in the specificity of the ^{99}Tc signal as a function of the mass resolution used. It was not possible to separate ^{99}Tc from polyatomic ions with a mass resolution of 300 (Fig.

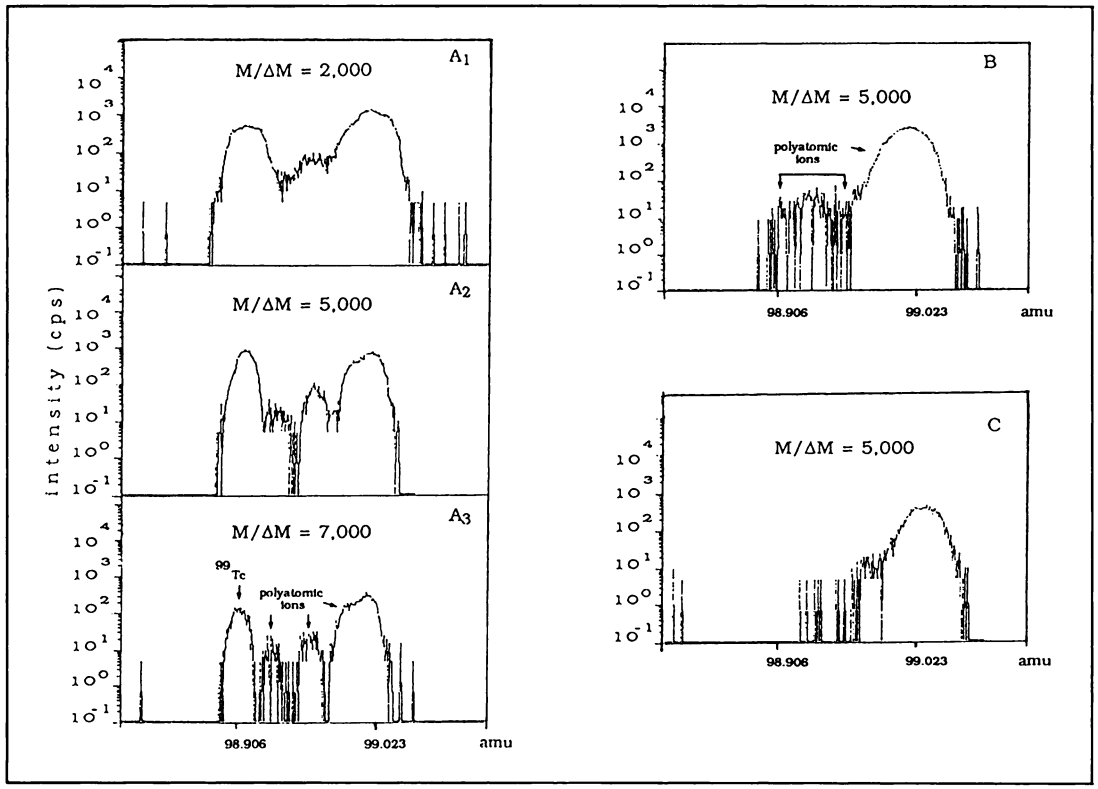

FIGURE 3. Mass spectra of ^{99}Tc introduced by HMPAO in leukocytes. (A) Pellet 1: ^{99}Tc-HMPAO-leukocyte. At M/DM = 2000 (A_1) the ^{99}Tc and polyatomic ion peaks are in a composite peak. At M/DM = 5000 (A_2), the ^{99}Tc (arrow one) and polyatomic ion peaks (arrow 2) are well separated and a higher mass resolution is not necessary (A_3). (B) Pellet 2: HMPAO-negative cell control. (C) Pellet 3: NaCl-negative cell control.

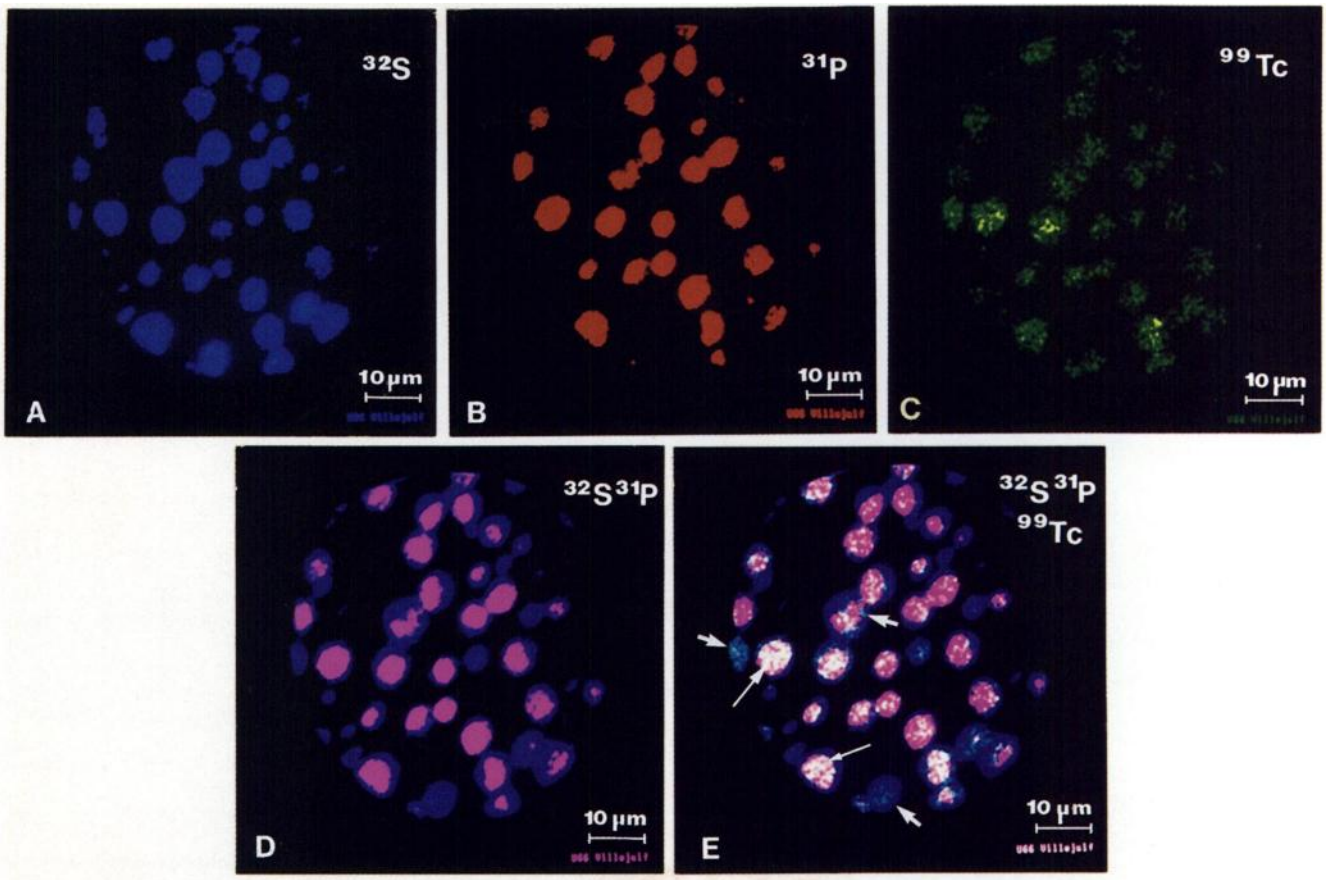

FIGURE 4. SIMS ^{99}Tc imaging. (A-B-C) Computerized images (pseudocolors) of sulfur (blue), phosphorus (red) and technetium (green) of leukocyte sections. By image processing, it is possible to superimpose these different images to produce a composite one. (D) Cell morphology was clearly depicted when the sulfur and phosphorus images were superimposed. (E) Technetium cellular distribution was visualized when sulfur, phosphorus and technetium images were superimposed. With the technique used, the nuclear technetium appears white (blue + red + green); the cytoplasmic technetium appears blue turquoise (blue + green). Large arrows show ^{99}Tc in the parts of the cytoplasm section without nuclear material. Sharp arrows show ^{99}Tc in the nuclear section.

2B); 2000 (Fig. 2C) seemed to be a more adequate mass resolution for the separation of major neighboring polyatomic ions in this macroaggregate matrix. Furthermore, the peak specific to Tc was not observed in the negative control sample (Fig. 2D).

Figure 3 shows the mass spectra obtained with sections from the three leukocyte pellets. In Pellet 1 (Fig. 3A, ^{99}Tc-HMPAO-leukocyte), a mass resolution of 2000 (Fig. 3A$_1$) was inadequate because additional peaks, which were not present in ^{99}Tc-AMA (Fig. 2C), appeared in this cell matrix. With a mass resolution of 5000, these new peaks were clearly visible in Pellet 2 (leukocyte-HMPAO) (Fig. 3B) but they were not detectable in Pellet 3 (leukocyte-NaCl) (Fig. 3C), nor in the reference sample without ^{99}Tc-HMPAO (Fig. 2D). With a mass resolution of 7000 (Fig. 3A$_3$), the ^{99}Tc peak was very well separated and no new polyatomic ions appeared. In practice, a mass resolution above 5000 guaranteed signal specificity for this cell matrix (Fig. 3A$_2$).

Technetium-99 Imaging

Figure 4 shows the elemental mapping of sections of embedded leukocytes labeled with ^{99}Tc-HMPAO. The sulfur image (Fig. 4A) displayed the proteic cell structures while the phosphorus image (Fig. 4B) visualized the nucleus because of its high DNA content. An image of cell morphology was obtained by the superimposition of these two images (Fig. 4D); the nucleus could be distinguished from the cytoplasm in this image. Figure 4C shows the ^{99}Tc image on the same image field and its superimposition with the sulfur and phosphorus images permitted the analysis of the cellular distribution of ^{99}Tc (Fig. 4E). Technetium labeling varied from one cell to another, some cells were heavily labeled, while others were not. Technetium-99 was present in all labeled cells in both the nucleus and the cytoplasm, as clearly shown in the parts of the section on the cytoplasm devoid of nuclear material.

DISCUSSION

Although numerous biological chemical elements have been detected by SIMS microscopy, technetium has never been studied with this technique. By using high mass resolution, we succeeded in detecting and localizing ^{99}Tc in tissue sections. Up to now, the microautoradiographic "track" method (*15,16*) has been employed to detect low

energy electrons of ^{99m}Tc, a metastable isomer which emits gamma and low-energy electrons (Auger electrons and internal conversion electrons). However, it is difficult to pinpoint the intracellular localization of ^{99m}Tc with the track method. SIMS microscopy demonstrated the heterogeneity of the inter- and intra-cellular distribution of ^{99}Tc in leukocytes. This method appears to be superior to microautoradiography because both ^{99}Tc (half-life 2.13 10^5 yr) and the ^{99m}Tc forms are detected, without any background, as is the case in microautoradiography.

A mass resolution of about 2000 was sufficient to avoid major polyatomic ion interferences with the ^{99}Tc reference sample. This was not the case for leukocytes labeled with ^{99}Tc-HMPAO (Pellet 1). A mass resolution of about 5000 was needed to circumvent these interferences because the chemical composition of the cell is more complex than that of albumin aggregates. Furthermore, mass spectra obtained from leukocytes labeled with HMPAO (Pellet 2), showed polyatomic ions which were not present in cells incubated with NaCl (Pellet 3). The new polyatomic ions introduced by the HMPAO solution were therefore exogenous in origin.

The nuclear and cytoplasmic distribution of ^{99}Tc in leukocytes, provided by SIMS microscopy, confirms the results obtained by two other methods. One of these methods, which employed cell disruption and isolation without imaging, indicated that ^{99m}Tc is localized between the nucleus and cytoplasm (*17*). The second, microautoradiography, demonstrated heterogeneous labeling from one cell to another (*18*) but was unable to verify the exact position in the cell. Our data show clearly that SIMS microscopy can pinpoint the distribution of the ^{99}Tc introduced by the radioligand in tissue.

A knowledge of the tissue distribution of radionuclides in tissue is essential for dosimetric studies, especially in metabolic radiotherapy. Unfortunately, the calculation of the absorbed dose is erroneously based on the assumption that the radioligand is homogeneously distributed throughout the target. Since the absorbed dose must be calculated at tissue level, knowledge of the biodistribution of the radioligand is essential. Our data indicate that SIMS microscopy is the method of choice for this evaluation. In addition, the study demonstrates that radioligands are not uniformly incorporated; some cells are heavily labeled whereas others are poorly labeled or not at all. The need to work at a high mass resolution increased signal specificity to the detriment of sensitivity. This may impede the study of the cellular distribution of ^{99}Tc after ^{99m}Tc in vivo injection (e.g., after immunoscintigraphy) under routine detection conditions with IMS 3F. However, the development of a SIMS sub-micron probe with a high extraction field and an optical transfer system allowing the collection and transfer of a maximum number of ions (*19*) should improve the ratio between selectivity and sensitivity and greatly facilitate the detection of ^{99}Tc and other radionuclides used in metabolic radiotherapy. In addition, one of the main interests of SIMS microscopy is its capacity to evaluate local element concentration (*20*). The local concentration of technetium is being investigated in our laboratory with this technique. This should constitute a new approach to cellular dosimetry.

ACKNOWLEDGMENTS

The authors thank Anne Petiet for assistance in the cell labeling and Colette Briançon for her suggestions for SIMS microscopy. The authors also thank Ms. Ingrid Küchenthal for her critical assessment and Lorna Saint-Ange for editing the manuscript.

REFERENCES

1. Masse R. Action of radiation on nuclear emulsions. *J Microscopy Biol Cell* 1976;27:83–90.
2. Rogers AW. *Techniques of autoradiography.* Amsterdam: Elsevier: 1979:429.
3. Trebbia P, Bonnet N. EELS elemental mapping with unconventional methods. 1. Theorical basis—image analysis with multivariate statistics and entropy concepts. *Ultramicroscopy* 1990;34:165–178.
4. Roomans. Introduction to x-ray microanalysis in biology. *J Electron Microscopy Technique* 1988;9:3–17.
5. Galle P. Tissue localization of stable and radioactive nuclides by secondary-ion microscopy. *J Nucl Med* 1982;23:52–7.
6. Burns MS. Biological microanalysis by secondary ion mass spectrometry: status and prospects. *Ultramicroscopy* 1988;24:269–82.
7. Chandra S, Morrisson G. Ion microscopy in biology and medicine. *Methods Enzymol* 1988;158:157–179.
8. Fragu P, Briançon C, Noël M, Halpern S. Imaging and relative quantification of ^{127}I in human thyroid follicle by analytical ion microscope: characterization of benign thyroid epithelial tumors. *J Clin Endocrinol Metab* 1989;69:304–309.
9. Briançon C, Halpern S, Telenczak P, Fragu P. Changes in ^{127}I mice thyroid follicle studied by analycal ion microscopy (AIM): a key for the comprehension of amiodarone-inducted thyroid diseases. *Endocrinology* 1990;127:1502–1511.
10. Fragu P, Briançon C, Fourré C, et al. SIMS microscopy in the biomedical field. *Biol Cell* 1992;74:5–18.
11. Peters AH, Osman S, Henderson BL, et al. Clinical experience with ^{99m}Tc hexamethylpropylene-amine oxime for labelling leucocytes and imaging inflammation. *Lancet* 1986;25:946–949.
12. Burns MS. Polyatomics interferences in high-resolution secondary ion mass spectra of biological tissue. *Anal Chem* 1981;53:2149–2152.
13. Truchet M. Etude de deux nouvelles méthodes d'analyse histologique: analyse élémentaire par émission ionique secondaire et analyse moléculaire par diffusion Raman. Thèse de doctorat d'état. Université Paris VI, 1982.
14. Olivo JC, Kahn E, Halpern S, Briançon C, Fragu P, Di Paola R. Microcomputer system for ion microscopy digital imaging and processing. *J Microscopy* 1989b;56:105–114.
15. Barbu H, Colas-Linhart N, Bok B. Technetium-99m autoradiography of labelled white cells. *Acta Haemat* 1984;71:13–17.
16. Wirquin E, Masse R, Meignan M. Microautoradiography of gamma-emitters interest of latensification progress. *Int J Appl Radiot Isot* 1984;35:489–493.
17. Costa DC, Lui D, Ell PJ. White cells radiolabeled with ^{111}In and ^{99m}Tc—a study of relative sensitivity and in vivo viability. *Nucl Med Commun* 1988;9:725–731.
18. de Labriolle-Vaylet CL, Colas-Linhart N, Petiet A, Bok B. Leucocytes marqués à l'HMPAO-^{99m}Tc: études fonctionnelles et microautoradiographiques. *J Med Nucl Biophys* 1990;14,2:137–141.
19. Slodzian G, Daigne B, Girard F, Boust F, Hillion F. Cartographie parallele de plusieurs elements ou isotopes par balayage avec une sonde ionique submicronique: premiers résultats. *C R Acad* 1990;(t.311, serie III):57–64.
20. Telenczak P, Ricard M, Halpern S, Fragu P. A method to evaluate the tissue absorbed dose in metabolic radiotherapy: preliminary results with MIBG. In: Benninghoven A, Evans C, McKeegan K, Storms H, Werner H, eds. *Secondary ion mass spectrometer SIMS VII.* Chichester: John Wiley and Sons Ltd; 1990:315–318.